AGU PUBLICATIONS

Geophysical Research Letters

RESEARCH LETTER

10.1002/2016GL069518

Key Points:
- The time elapsed since the last eruption overruns the recurrence time in the last 100 kyr
- Maximum uplift rates (>2 mm/yr) are concetrated in the area hosting the most recent (<200 ka) vents
- We suggest that the observed uplift might be the result of magma injection within the youngest plumbing system of the volcano

Supporting Information:
- Supporting Information S1
- Table S1
- Data Set S1

Correspondence to:
F. Marra,
fabrizio.marra@ingv.it

Citation:
Marra, F., M. Gaeta, B. Giaccio, B. R. Jicha, D. M. Palladino, M. Polcari, G. Sottili, J. Taddeucci, F. Florindo, and S. Stramondo (2016), Assessing the volcanic hazard for Rome: $^{40}Ar/^{39}Ar$ and In-SAR constraints on the most recent eruptive activity and present-day uplift at Colli Albani Volcanic District, *Geophys. Res. Lett.*, *43*, 6898–6906, doi:10.1002/2016GL069518.

Received 8 APR 2016
Accepted 13 JUN 2016
Accepted article online 15 JUN 2016
Published online 12 JUL 2016

Assessing the volcanic hazard for Rome: $^{40}Ar/^{39}Ar$ and In-SAR constraints on the most recent eruptive activity and present-day uplift at Colli Albani Volcanic District

F. Marra[1], M. Gaeta[2], B. Giaccio[3], B. R. Jicha[4], D. M. Palladino[2], M. Polcari[1], G. Sottili[3], J. Taddeucci[1], F. Florindo[1], and S. Stramondo[1]

[1]Istituto Nazionale di Geofisica e Vulcanologia, Rome, Italy, [2]Dipartimento di Scienze della Terra, Sapienza, Università di Roma, Rome, Italy, [3]Istituto di Geologia Ambientale e Geoingegneria - CNR, Rome, Italy, [4]Department of Geoscience, University of Wisconsin-Madison, Madison, Wisconsin, USA

Abstract We present new $^{40}Ar/^{39}Ar$ data which allow us to refine the recurrence time for the most recent eruptive activity occurred at Colli Albani Volcanic District (CAVD) and constrain its geographic area. Time elapsed since the last eruption (36 kyr) overruns the recurrence time (31 kyr) in the last 100 kyr. New interferometric synthetic aperture radar data, covering the years 1993–2010, reveal ongoing inflation with maximum uplift rates (>2 mm/yr) in the area hosting the most recent (<200 ka) vents, suggesting that the observed uplift might be caused by magma injection within the youngest plumbing system. Finally, we frame the present deformation within the structural pattern of the area of Rome, characterized by 50 m of regional uplift since 200 ka and by geologic evidence for a recent (<2000 years) switch of the local stress-field, highlighting that the precursors of a new phase of volcanic activity are likely occurring at the CAVD.

1. Introduction

Assessing the volcanic eruption hazards in densely populated areas is of primary importance for correctly evaluating the risks and thus designing proper emergency plans for civil protection purposes. This relies on the knowledge of a number of volcanological processes and physical parameters including the eruptive history (e.g., styles of eruptive events and their time recurrence) and the current surface deformations, all of which are of paramount importance. The southeastern suburbs of the City of Rome extend onto the gentle slopes of the Colli Albani Volcanic District (CAVD), the eruptive history of which spans between 608 ka and 36 ka [*Karner and Renne*, 1998; *Karner et al.*, 2001a; *Marra et al.*, 2003; *Freda et al.*, 2006; *Giaccio et al.*, 2009; *Marra et al.*, 2009; *Gaeta et al.*, 2011, 2016]. The almost regular temporal recurrence of ~45 kyr (periodicity coefficient $Cv = 0.38$) for the 11 eruptive periods during the whole CAVD history allowed in the past to asses a quasi-cyclical eruptive behavior [*Marra et al.*, 2004a]. More recently, based on an updated geochronological data set [*Gaeta et al.*, 2016], the weighted average recurrence period for these eruptive cycles has been better constrained to 44.6 ± 1.5 kyr, along with the weighted average dormancy of 38.8 ± 1.5 kyr, defined as the time elapsed between the end of an eruptive cycle and the start of the successive one.

Notably, the time elapsed since the start of the last eruptive cycle (41 ka [*Freda et al.*, 2006]) and the dormancy duration since its end (36 kyr [*Freda et al.*, 2006; *D'Ambrosio et al.*, 2010]) are on the same order of those characterizing the whole eruptive history, thus evidencing that the CAVD is a dormant, rather than extinct, volcano.

The quasiperiodic eruptive behavior with an average recurrence time of ~45 kyr has been statistically assessed for the whole Roman Comagmatic Province by *Marra et al.* [2004a], who made two working hypothesis to explain the regular duration of the eruptive cycles: (i) progressive weakening up to strength failure in the crust due to magma underplating and (ii) cyclic injection of convective plumes into the mantle wedge. Moreover, the peculiar behavior of the CAVD in which almost absolute dormancies separate each eruptive cycle, as opposed to a more continuous activity at the other volcanic districts of the Tyrrhenian Sea Margin, has been related to the prevalence of a local transpressive stress field characterized by horizontal NE-SW trending $\sigma 1$, over a regional extensional one, causing sealing of the preferential pathways for magma uprising represented by the NW-SE trending faults [*Marra et al.*, 2009]. Widespread geologic evidence of alternating tectonic regimes with diffuse right-lateral N-S faulting and associated ~E-W trending conjugated systems of transcurrent faults

superposing NW-SE trending normal faults has been documented in the CAVD and the Rome area [*Faccenna et al.*, 1994a, 1994b; *Marra*, 1999, 2001; *Marra et al.*, 2004b]. Triggering of the high explosive eruptive cycles at the CAVD has been related with stress-field switching from transpression to extension [*Frepoli et al.*, 2010].

Regional uplift of ~45 m in the last 250 kyr has been interpreted to reflect magma injection in the upper crust, similar to equivalent uplifts that occurred around 800 ka and 600 ka at the onset of volcanic activities at Monti Sabatini Volcanic District, located NW of Rome, and CAVD, respectively [*Karner et al.*, 2001b]. In recent years, a seismic swarm affecting the Colli Albani area in 1990–1991 has been related to a local uplift of ~50 cm that has occurred since the 1960s as evidenced by geodetic data [*Amato and Chiarabba*, 1995a]. Based on teleseismic tomography by *Cimini et al.* [1994], evidencing a low-velocity zone between 5.0 and 10.5 km of depth centered below the craters of Ariccia and Nemi (Figure 1), *Amato and Chiarabba* [1995a] hypothesized the presence of a hot crustal body, possibly a magma chamber, responsible for the observed decrease (5%) of seismic velocity. Finally, interferometric synthetic aperture radar (InSAR) data for the time span 1993–2000 revealed up to 2.6 mm/yr of active uplift along the west margin of Colli Albani caldera, a further indication of magma injection and potential volcanic unrest [*Salvi et al.*, 2004].

In this paper, we provide further chronological data for the most recent volcanic activity coupled with new InSAR data for the CAVD area, which better constrain its temporal recurrence and vent areas and the current surface deformations of the volcanoes. These data provide evidence for a clear correspondence between the location of the most recent eruptive centers (i.e., younger than 200 ka) and the sector characterized by ongoing uplift, highlighting that the signals of a new phase of volcanic activity are likely occurring at the CAVD.

2. Geological Background

The CAVD is part of the Roman Magmatic Region, a NW-SE chain of ultrapotassic volcanic districts which developed along the Tyrrhenian Sea margin of central Italy during the Middle Pleistocene (Figure 1) [*Peccerillo*, 2005]. Its eruptive history has been subdivided into three main phases of activity characterized by decreasing magma volumes and energy of eruptions [*De Rita et al.*, 1988, 1995; *Giordano et al.*, 2006]: (1) the Tuscolano-Artemisio Phase (TA; 608–351 ka), recently further distinguished into early- and late-TA, which consisted of individual caldera-forming events up to a few tens of km^3 in volume (dense rock equivalent (DRE)), (2) the Monte delle Faete Phase (MdF; 309–241 ka) characterized by Strombolian and effusive activity, and (3) the recent eruptive activity (younger than 200 ka), further distinguished into a Late Hydromagmatic Phase (LHP; 204–142 ka) and the Albano Phase (69–36 ka) [*Marra et al.*, 2009; *Gaeta et al.*, 2016]. Specifically, the recent eruptive history is characterized by variable magmatic and hydromagmatic activity styles from several eccentric, both monogenetic and polygenetic, maars (Figure 1), with erupted volumes in the order of 0.1–1 km^3 DRE for individual eruptive events [*Sottili et al.*, 2009]. With respect to previous LHP activity, the most recent activity of the polygenetic Albano Maar shows increased intensity and magnitude [*Freda et al.*, 2006; *Giaccio et al.*, 2007; *Sottili et al.*, 2008; *Giaccio et al.*, 2009], being not limited to short-reaching phreatomagmatic explosions, but also including far-reaching pyroclastic density currents and high, sustained eruption columns, up to Sub-plinian in intensity [*Giaccio et al.*, 2007; *Sottili et al.*, 2009].

3. Methods

3.1. Samples Collection and Selection

In this work, a new set of samples was collected in order to conclusively assign ephemeral products of the CAVD to the established activity phases. Indeed, part of the hydromagmatic centers previously attributed to the recent activity phase has been shown to be instead part of the older TA and MdF phases [*Gaeta et al.*, 2016]. Assessing the eruption ages for several of ephemeral centers can be problematic, since xenocrystic contamination in hydromagmatic products, in which the juvenile fraction may be reduced or even lacking, is a common occurrence. Indeed, pervasive contamination from older magma (i.e., the 365 ± 4 ka magma of the Villa Senni eruption cycle) was evidenced in several younger hydromagmatic products analyzed in *Marra et al.* [2003] and *Gaeta et al.* [2016]. Bearing in mind these potential problems, we have conducted new sampling of the volcanic centers yielding stratigraphically inconsistent or doubtful age results in previous studies. The selected samples have been subjected to $^{40}Ar/^{39}Ar$ dating experiments, taking into account their key textural petrographic features, aimed at better defining the CAVD eruptive history, with particular focus on assessing the ages of the most recent eruptions and their recurrence time.

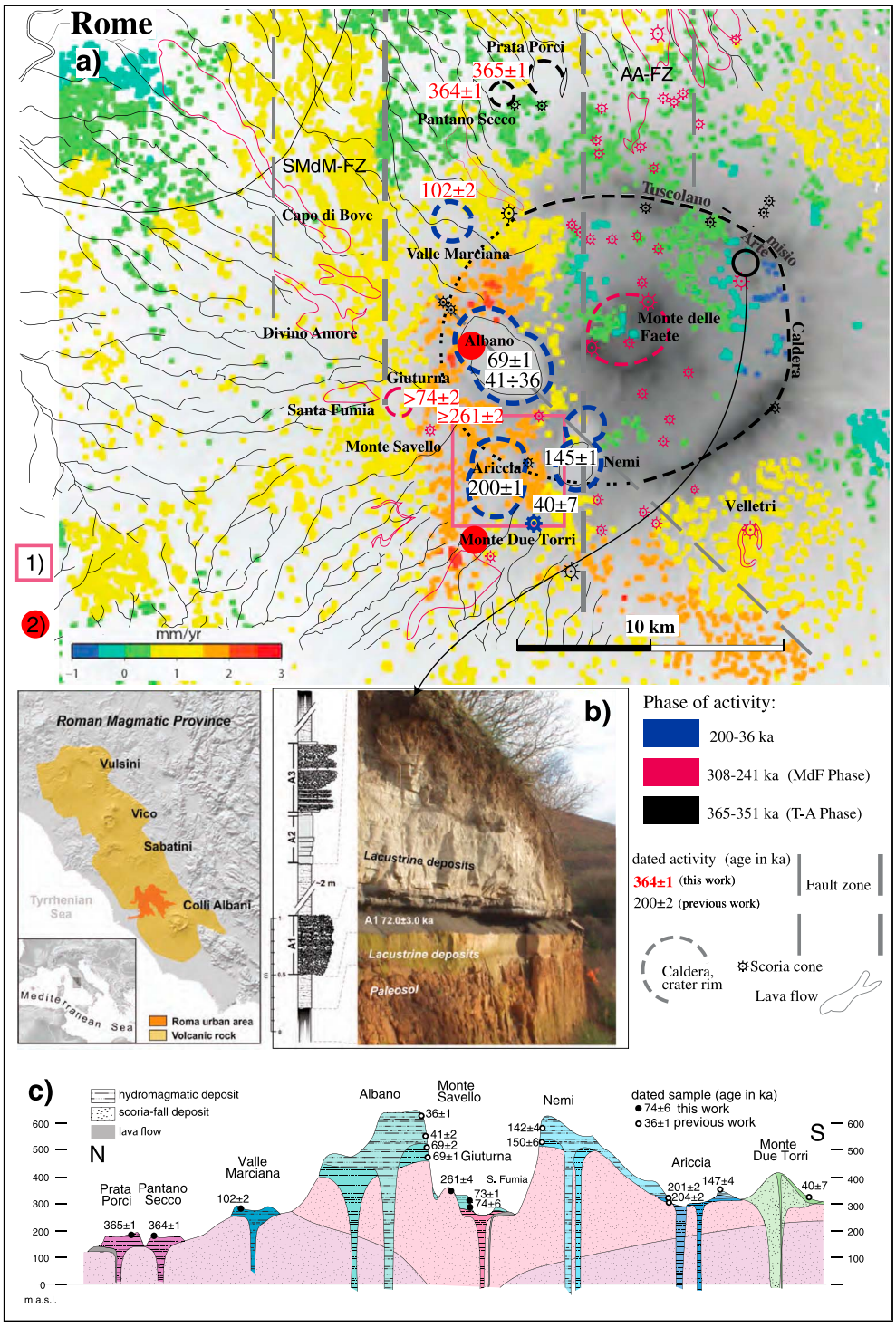

Figure 1. Reference maps and summary of the main results. (a) Map of CAVD showing location of the hydromagmatic centers, principal scoria cones, and lava flows. Temporal range of activity of the vents is assessed based on previous literature data and on the new $^{40}Ar/^{39}Ar$ age constraints provided in this work. Interferometric Point Target Analysis (IPTA) velocity map resulting from the 2003 to 2010 SAR data relative to the investigated area is also shown. The highest uplift rates (>2 mm/yr) concentrate within a N-S stretching area comprised between the Santa Maria delle Mole Fault Zone (SMdM-FZ) and the Acque Albule Fault Zone (AA-FZ), in the same sector where the vents of the most recent volcanic activity (<200 ka; blue crater rims) are located. (1) *P* waves low-velocity zone between 5.0 and 10.5 km depth detected by teleseismic topography in *Cimini et al.* [1994]. (2) Mogi sources at 5 and 7 km depth obtained by ascending and descending *PS* ground velocities modeling in *Salvi et al.* [2004]. (b) Picture and stratigraphic log showing the first three Albano units (A1 to A3) within lacustrine deposits directly lying on a deep reddish paleosol [from *Giaccio et al.*, 2009]. (c) N-S composite cross-section showing the stratigraphic relationships of the hydromagmatic centres and other key-products, and the location of the samples dated with $^{40}Ar/^{39}Ar$ method, constraining the most recent phase (< 365 ka bp) of volcanic activity. Horizontal not to scale.

Selected deposits for $^{40}Ar/^{39}Ar$ age determination include (Figure 1) the following:

Prata Porci (previously assessed age $\leq 279 \pm 6$ ka [*Gaeta et al.*, 2016]);
Pantano Secco (previously assessed age 364 ± 2 ka [*Marra et al.*, 2003]);
Valle Marciana (previously assessed age 365 ± 2 ka [*Marra et al.*, 2003]);
Giuturna (previously assessed age $\leq 72 \pm 2$ ka [*Marra et al.*, 2003]); and
Monte Savello (previously undated).

In addition, in order to obtain indirect chronological constrains, based on the time-dependent trends of $^{87}Sr/^{86}Sr$ and $^{143}Nd/^{144}Nd$ analysis [e.g., *Gaeta et al.*, 2006; *Giaccio et al.*, 2013], we also present previously unpublished Sr and Nd isotope ratios performed by *Gaeta et al.* [2016; see methods in this paper], for the Santa Fumia lava flow (AH37; Figure 1a), cropping out on the western flanks of the Giuturna crater rim, whose temporal relationship with the hydromagmatic activity of this maar was previously not firmly established.

3.2. $^{40}Ar/^{39}Ar$ Geochronology

Leucite and occasional sanidine crystals were isolated from the deposits via standard magnetic and density separation techniques. Groundmass from the lava at Prata Porci was hand-picked under a binocular microscope to ensure that all phenocrysts were removed. The samples were irradiated in the CLICIT facility at the Oregon State University TRIGA reactor and were monitored with the 1.1864 Ma Alder Creek sanidine [*Rivera et al.*, 2013; *Jicha et al.*, 2016]. Single-crystal total fusion analyses were performed with a Photon Machines Fusions 60 W CO_2 laser. All argon isotopic analyses were done using a Noblesse 5 collector mass spectrometer following the procedures of *Jicha et al.* [2016].

3.3. InSAR Data

The InSAR data set consists in 117 Single Look Complex SAR images provided by the European Space Agency satellites ERS 1-2, from 1993 to 2002, and from Envisat spanning 2003 to 2010. The satellite data (at C-band, $f \sim 5.3$ GHz) were acquired along descending orbit with an incidence angle of about 23° and an azimuth angle of $\sim -163°$. Although provided by different satellites, the data were jointly processed because of the same viewing geometry, acquisition mode, and frequency band. Multilook factors of 4 by 20 were applied along range and azimuth direction achieving a pixel posting of $\sim 80 \times 80$ m.

The Multi-Baseline Interferometric Point Target Analysis (IPTA) approach of the GAMMA software [*Werner et al.*, 2003] has been applied to perform the resulting 261 interferograms, obtained thanks to applying the maximum perpendicular and temporal baseline set to 300 m and 600 days, respectively. The topographic contribution in the interferometric phase was removed by using the digital elevation model provided by the Shuttle Radar Topography Mission mission, while spatial filtering and temporal filtering were applied in order to reduce the atmospheric contribution.

Finally, the interferograms affected by problems such as unwrapping phase jumps, uncompensated atmosphere, and lack of coherence were discarded from the processing.

4. Results

4.1. Petrographic and Textural Features of the Dated Volcanic Deposits

4.1.1. Prata Porci: AH8-F2

The AH8-F2 lapilli show a porphyritic, weakly vesiculated (<5 vol %) texture made up of submillimeter sized (up to 500 μm) leucite, clinopyroxene, and magnetite phenocrysts surrounded by a glassy to holocrystalline groundmass. Leucite, the most abundant phenocryst (20 vol %), is euhedral, with the typical trapezohedral habit. Clinopyroxene (5 vol %) is euhedral and characterized by elongate/acicular habit. The groundmass is made up of glass that frequently is turned to zeolites. The textural features of the AH8-F2 lapilli are clearly primary, and different from those of the Pozzolanelle scoria clasts, originated from a magma-water interaction process. Large leucite crystals (400–500 μm sized) were extracted from the scoria for the $^{40}Ar/^{39}Ar$ age determination.

4.1.2. Pantano Secco: AH12-B1

A single, 2 cm sized scoria fragment, used for the petrographic evaluation of the AH12-B1 sample, shows relatively coarse (up to 500 μm) leucite, clinopyroxene, and mica crystals surrounded by a scarcely vesicular (5 vol %) groundmass. Leucite, the most abundant microphenocryst (25 vol %), is euhedral, with the typical

Table 1. Geochronology

Eruptive Center	Sample	Age (ka) ±2σ
Prata Porci	AH8-F2	365.3 ± 1.2
Pantano Secco	AH12-B1	364.5 ± 1.2
Monte Savello	MS2	261.1 ± 3.7 (three youngest crystals)
Valle Marciana	AH10-C	102.0 ± 1.6
Giuturna	G3	73.6 ± 1.3
Giuturna	G4	74.4 ± 3.3 (three youngest crystals)

trapezohedral habit. Clinopyroxene (10 vol %) and mica (<5 vol %) are euhedral and sometimes characterized by elongate/acicular habit (in particular the mica crystals). The groundmass is made up of clinopyroxene + leucite and glass turned to zeolites and compatible with an origin from a magma-water interaction process, even if the occurrence of mica indicates a more differentiated magmas respect those have fed *Prata Porci* eruption determination.

4.1.3. Valle Marciana: AH10-C

Sample AH10-C (a single rock fragment of 2.5 cm in diameter) shows a porphyritic and vesicular texture, formed by abundant olivine and clinopyroxene phenocrysts (20 vol %) and scarce subrounded vesicles (5 vol %). Olivine crystals are submillimeter-sized, euhedral to subhedral, that frequently include Cr-spinels and sometimes form crystal clots. Clinopyroxenes are subhedral, millimeter- to submillimeter-sized (up to 5 mm). The groundmass is made up of olivine + clinopyroxene + leucite and scarce glass and lacks late magmatic phases. In particular, the absence of oxides in the groundmass represents a rarity to the district scale.

4.1.4. Giuturna: G3

Sample G3 (a single, 3.5 cm sized rock fragment) shows a pyroclastic texture formed by (i) submillimeter-sized, leucite-rich, and scarcely vesicular juveniles; (ii) submillimeter-sized phenoclasts, and (iii) relatively abundant ash matrix (>50 vol %). Phenoclasts include in order of abundance: leucite, clinopyroxene, phlogopite, and rare feldspars, oxide, apatite, and garnet. Noteworthy, the absence of calcite and the textural features of the juveniles in the G3 sample are analogous to those of the uppermost volcanic deposits of the first cycle of activity of the Albano maar (i.e., cf. sample AH3C8 described by *Freda et al.* [2006]).

4.1.5. Giuturna: G4

Sample G4 (a single, 3 cm-sized rock fragment) shows a pyroclastic texture made up of (i) olivine-bearing, millimeter-sized, and scarcely vesicular juveniles; (ii) olivine, clinopyroxene, leucite, garnet, and green spinel phenoclasts; (iii) granular and carbonate lithic clasts; and (iv) scarce ash matrix. Noteworthy, the association of olivine, igneous, and thermometamorphic hypoabissal rocks, garnet, and green spinel is also typical of the volcanic deposits occurring at the base of the first cycle of activity of the Albano maar [*Freda et al.*, 2006; *Gaeta et al.*, 2009; *Di Rocco et al.*, 2012].

4.1.6. Monte Savello: MS2

A single rock fragment (3 cm sized) was impregnated prior to thin section preparation because the MS2 sample was weakly lithified. The thin section shows an ash-rich, clastic texture characterized by the abundance of sanidine and the absence of leucite. Notably, sanidine is virtually lacking among CAVD products [e.g., *Gozzi et al.*, 2014], whereas leucite is ubiquitary, thus clearly indicating a reworked origin for the MS2 sample, probably from Monti Sabatini, sanidine-rich, fallout products.

4.2. $^{40}Ar/^{39}Ar$ and Sr-Nd Isotope Data

$^{40}Ar/^{39}Ar$ ages for the analyzed samples are reported in Table 1 with 2σ analytical unceratinites (full analytical data in Table S1 in the supporting information). Location of the samples and stratigraphic relationships of the dated products are shown in the cross section of Figure 1c. Eruption ages of 364.5 ± 1.2 ka, 365.3 ± 1 ka, and 102.0 ± 1.6 ka are assessed for Pantano Secco, Prata Porci, and Valle Marciana centers, respectively, based on the straightforward juvenile features of the dated samples, as evidenced by petrographic analysis. We consider the age of 261.1 ± 3.7 ka yielded by three youngest crystals within an extremely scattered population with dates up to 1087 ka, as a postquem for the activity of the Monte Savello scoria cone. The sample collected on the flanks of the edifice is evidently a reworked colluvial deposit; however, the youngest crystals are likely derived from the primary scoria-fall deposit. Moreover, the lack of younger crystals allows us to constrain Monte Savello within the diffused scoria-cone activity during the MdF phase (308–241 ka [*Gaeta et al.*, 2016]).

Ages of 74.4 ± 3.3 and 73.6 ± 1.3 ka, as well as idiosyncratic lithological features of the two pyroclastic-surge deposits separated by a faintly developed paleosoil cropping out within the inner rim of the Giuturna crater (samples G4 and G3), strongly suggest that they match the two major eruptive units of the first cycle of

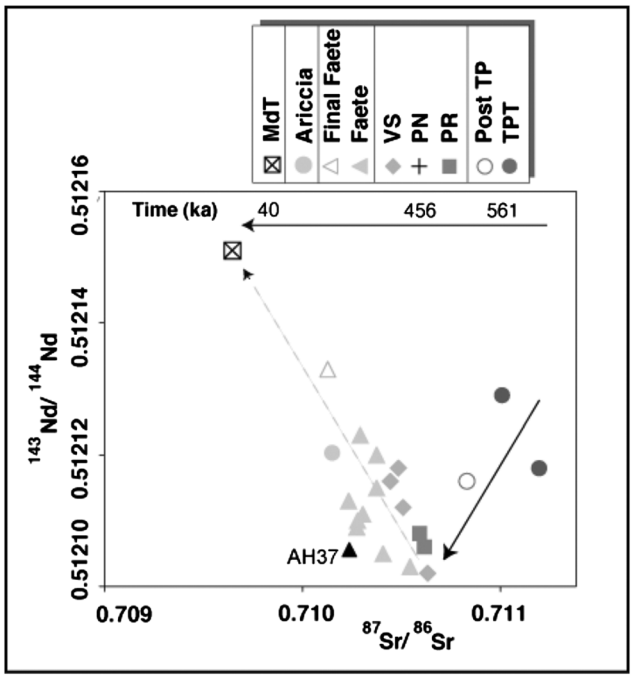

Figure 2. The $^{87}Sr/^{86}Sr$ versus $^{143}Nd/^{144}Nd$ composition of the Santa Fumia lava flow (sample AH37), plotted in the diagram showing the temporal variations for the CAVD magmas [*Gaeta et al.*, 2016], consistently indicates its attribution to the Monte delle Faete phase of activity.

Albano, i.e., A1 and A3 dated to 72.0 ± 3.0 and 73.0 ± 3.0 ka [*Giaccio et al.*, 2009], whose very proximal counterparts are dated 68.9 ± 0.2 ka and 68.6 ± 1.1 ka (±1σ), respectively [*Freda et al.*, 2006]. Therefore, the Giuturna crater formed before 70 ka and was successively partially filled by the eruptive deposits of Albano.

Consistently, the $^{87}Sr/^{86}Sr$ and $^{143}Nd/^{144}Nd$ analyses of the Santa Fumia lava sample, whose vent area coincides with the Giuturna crater (Figure 1a), yielded values of 0.710239 and 0.512105, respectively (Figure 2), which are in the range of the MdF phase (Figure 2). Therefore, we suggest that the Giuturna poligenetic center belongs this phase of activity, an inference which is also consistent with its proximity to the inferred source of the major Divino Amore and Capo di Bove lava flows also erupted in the 308–241 ka interval [*Marra et al.*, 2003].

4.3. InSAR

The results from InSAR analysis are shown in Figure 1a. The retrieved surface deformation trend highlights a clear uplifting area mainly located west the Albano and Nemi lakes. Indeed, the mean line of sight deformation registered in this area is larger than 1.5 mm/yr and peaks at around 2.5 mm/yr close to the northwestern rim of the Albano crater. Another uplifiting zone with slight lower deformation rates, i.e., 0.5–1 mm/yr, is observed southwest of the small town of Velletri, and its spatial distribution is tentatively correlated with a buried NW-SE normal fault. Future analysis will be focused on understanding the volcanic source mechanism producing this surface displacement field. Furthermore, a small subsiding area (~ −1.3 mm/yr) is observed in the eastern part of the TA caldera, most likely ascribable to local water pumping activity. Finally, a significant subsidence of about 2 mm/yr is also produced in the city of Rome, surrounding the Tiber River valley because of an already known phenomenon of sediment compaction [*Stramondo et al.*, 2008].

The observed deformation pattern is in good agreement with that previous depicted for the earlier time span (1993–2000) by *Salvi et al.* [2004]. The longer time interval analyzed here allows us to detect the temporal continuity of the uplift phenomenon at least until the 2010, revealing an ongoing almost linear deformation trend.

5. Discussion and Conclusions

The eruptive centers hosting the most recent phase of activity since 200 ka are located on the western edge of the Tuscolano-Artemisio caldera, within a N-S stretching sector bounded by the two major tectonic structures of Santa Maria delle Mole (SMdM) and Acque Albule (AA) Fault Zone [*Marra*, 2001; *Frepoli et al.*, 2010] (Figure 1). These correspond to vertical N-S crustal discontinuities, originated as right-lateral transcurrent faults, which are re-activated as left-lateral, transtensional faults under the present-day NE-oriented extensional regime [*Frepoli et al.*, 2010]. Remarkably, the vents of major lava flows erupted during the MdF phase are located along these deep tectonic lineaments, which acted as preferential pathways for uprising of magma feeding effusive eruptions. In contrast, the vents of the hydromagmatic activity concentrate in the fractured crustal blocks within the N-S discontinuities [*Marra*, 1999, 2001], which correspond to structural

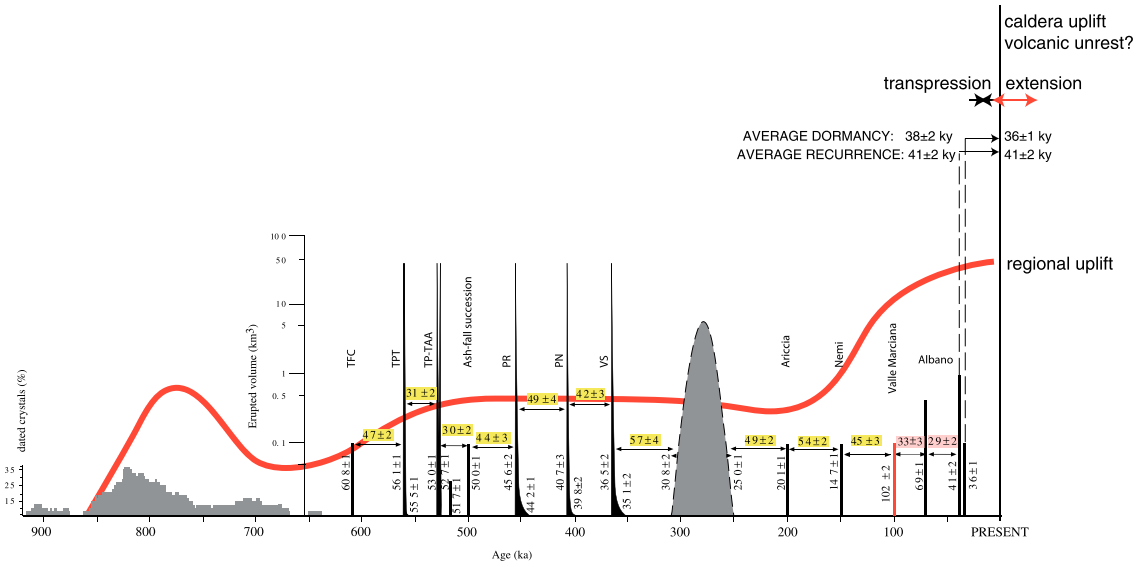

Figure 3. Comparison of the regional uplift (red line [*Karner et al.*, 2001b]) and the eruptive history of the CAVD (the vertical bars represent the eruptive cycles in the 608–36 ka time interval; the ideogram represents statistical assessment of the eruptive activity in the interval 900–650 ka; modified from *Marra et al.* [2009]). Individual dormancies separating the eruptive cycles, used to compute the average recurrence time, are reported (yellow boxes). The newly assessed eruption age of 102 ± 2 ka for Valle Marciana suggests a shorter recurrence time of ~31 kyr (red boxes) for the eruptive activity in the last 100 ka, with respect to 45 kyr for the previous 500 ka.

highs of the carbonate substrate [*Funiciello and Parotto*, 1978]. The explosive activity since 200 ka has been interpreted as a new volcanic phase, related to a prevalently extensional tectonic regime, with respect to the previous TA phase and MdF phase, which appears dominated by the transpressive regime that alternated with the extensional one in the area of Rome [*Marra et al.*, 2009; *Frepoli et al.*, 2010].

Figure 1a shows that the sector characterized by the highest uplift rates (>2 mm/yr) is also constrained between the two N-S fault zones, thus overlapping the source vent area of the most recent eruptive activity and suggesting that the observed uplift might be the result of magma emplacement within this crustal block. Geological evidence from the TA caldera also suggests the occurrence of deformation related to the Albano eruptive activity (Figure 1b). In this area, a several meter-thick lacustrine succession, directly lying on a deep reddish paleosol, contains the first three units of Albano (A1 to A3, ~70 ka), with A1 occurring very close the base of the lake sediments [*Giaccio et al.*, 2009] (Figure 1b). This indicates that slightly before the A1 eruption, the previously drained caldera floor (i.e., as recorded by the paleosol), hosted, over the whole early stage of Albano activity, a lacustrine environment, conceivably due to a significant uplift just before the onset Albano eruptive activity which caused the damming of the western edge of the TA caldera.

The possibility that the observed uplift may be due to magma injection under the TA caldera has been evaluated by *Salvi et al.* [2004], who, based on the ESR SAR data collected in the years 1993–2000, modeled the ascending and descending *PS* ground velocities to constrain source models for the total inflation observed in the 8 year period. These authors obtained a best fit with two Mogi sources aligned in a N-S direction at 5 and 7 km depth beneath the Albano and 2 km south of the Ariccia craters, respectively, consistent with the presence of a *P* waves low-velocity zone at this depth evidenced by teleseismic tomography by *Cimini et al.* [1994] (Figure 1a). Our results from InSAR analysis extended over the time interval 1993–2010 reported in Figure 1 are in substantial agreement with previous results by *Salvi et al.* [2004], either in rate amplitude and spatial distribution; therefore, we assume that the observed uplift is consistent with geometry and location of the sources modeled by these authors, while we address to future work a more detailed modeling.

The age of ~100 ka provided here to the Valle Marciana center defines a 31 ± 1.7 kyr weighted average recurrence period in the most recent volcanic activity (Figure 3), indicating an intensification of the eruptive activity parallel to the regional uplift acting since 200 ka. Thus, the time elapsed since the last eruption cycle, 36 ± 1 kyr, overruns the average recurrence time for the activity of the last 100 kyr, supporting the hypothesis that magmatic inflation is in act. Moreover, when the average recurrence and the average dormancy periods are re-assessed over the 600 kyr to present time span based on the newly detected eruption cycle at Valle Marciana, the values

of 41 ± 2 kyr and 38 ± 2 kyr are found, with respect to an identical time of 41 ± 2 ka and a same order dormancy of 36 ± 1 kyr elapsed since the start of he last eruptive cycle at Albano (Figure 3).

We also remark that consistent with assumptions that the cycles of the magma chambers recharge are tectonically triggered by the subduction-related extensional process acting in this region, *Frepoli et al.* [2010] have hypothesized that uprising of a new batch of magma is able to trigger a stress-field permutation below the CAVD, causing the regional extensional regime to supersede the local transpressive regime, and leading to the initiation of a new eruptive cycle. The occurrence of a stress-field switch in historical time is suggested by geophysical indicators (i.e., earthquakes and borehole breakouts) showing a present-day stress-field characterized by a NE striking $\sigma 3$ [*Amato and Chiarabba*, 1995b; *Montone et al.*, 1995; *Frepoli et al.*, 2010], as opposed to structural-geologic data evidencing widespread occurrence of transpressive faulting affecting terrains as young as 25 ka [*Faccenna et al.*, 1994a, 2008; *Marra*, 1999, 2001], as well as tectonic deformation affecting a II century CE Roman aqueduct system, linked to a NE striking $\sigma 1$ [*Florindo et al.*, 2004; *Marra et al.*, 2004b].

In light of all the above-mentioned indicators, including (i) the very recent switch in the tectonic regime after a 200 kyr long uplift phase of ~50 m, (ii) the time elapsed since the last eruptive cycle at CAVD equal to the overall average recurrence and overrunning the average dormancy of 31 kyr that characterized the $<$100 kyr activity (Figure 3), and (iii) the coincidence between the sector presently characterized by $>$2 mm/yr uplift and the location of the eruptive centers that were active in the last 200 kyr (Figure 1a), there is a clear convergence of independent pieces of evidence suggesting the onset of a new volcanic cycle, possibly leading to eruptive unrest that may affect the area of Rome.

Acknowledgments
We thank two anonymous reviewers and Guido Ventura for their useful suggestions. Full $^{40}Ar/^{39}Ar$ analytical data are provided in Table S1.

References

Amato, A., and C. Chiarabba (1995a), Earthquake occurrence and crustal structure, in *The Volcano of the Alban Hills*, edited by R. Trigila, pp. 193–211, Univ. degli Studi di Roma "La Sapienza", Roma.

Amato, A., and C. Chiarabba (1995b), Recent uplift of the Alban Hills Volcano (Italy): Evidence of magmatic inflation?, *Geophys. Res. Lett.*, *22*, 1985–1988, doi:10.1029/95GL01803.

Cimini, G. B., C. Chiarabba, A. Amato, and H. M. Iyer (1994), Large teleseismic P-wave residual variation in the Alban Hills volcano, central Italy, *Ann. Geofis.*, *37*, 969–988.

D'Ambrosio, E., B. Giaccio, L. Lombardi, F. Marra, M. F. Rolfo, and A. Sposato (2010), L'attività recente del centro eruttivo di Albano tra scienza e mito: Un'analisi critica del rapporto tra il vulcano laziale e la storia dell'area albana, in *Lazio e Sabina, Sesto Incontro di Studi sul Lazio e Sabina, Roma*, pp. 125–136, Soprintendenza per i Beni Archeologici del Lazio, Roma.

de Rita, D., R. Funiciello, and M. Parotto (1988), Carta geologica del Complesso vulcanico dei Colli Albani, Progetto Finalizzato 'Geodinamica' C.N.R., Rome, Italy.

de Rita, D., C. Faccenna, R. Funiciello, and C. Rosa (1995), Stratigraphy and volcano-tectonics, in *The Volcano of the Alban Hills*, edited by R. Trigila, pp. 33–71, Univ. degli Studi di Roma "La Sapienza", Roma.

Di Rocco, T., C. Freda, M. Gaeta, S. Mollo, and L. Dallai (2012), Magma chambers emplaced in carbonate substrate: Petrogenesis of skarn and cumulate rocks and implication on CO2-degassing in volcanic areas, *J. Petrol.*, *53*, 2307–2332.

Faccenna, C., R. Funiciello, P. Montone, M. Parotto, and M. Voltaggio (1994a), An example of late Pleistocene strike-slip tectonics: The Acque Albule basin (Tivoli, Latium), *Mem. Descr. Carta Geol. Ital.*, *49*, 37–50.

Faccenna, C., R. Funiciello, and M. Mattei (1994b), Late Pleistocene N-S shear zones along the Latium Tyrrhenian margin: Structural characters and volcanological implications, *Boll. Geofis. Teor. Appl.*, *36*, 507–522.

Faccenna, C., M. Soligo, A. Billi, L. De Filippis, R. Funiciello, C. Rossetti, and P. Tuccimei (2008), Late Pleistocene depositional cycles of the Lapis Tiburtinus travertine (Tivoli, Central Italy): Possible influence of climate and fault activity, *Global Planet. Change*, *63*, 299–308, doi:10.1016/j.gloplacha.2008.06.006.

Florindo, F., F. Marra, P. Montone, M. Pirro, and E. Boschi (2004), Palaeomagnetic results from an archaeological site near Rome (Italy): New insights for tectonic rotation during the last 0.5 Ma, *Ann. Geophys.*, *47*(5), 1665–1673.

Freda, C., M. Gaeta, D. B. Karner, F. Marra, P. R. Renne, J. Addeucci, P. Scarlato, J. Christensen, and L. Dallai (2006), Eruptive history and petrologic evolution of the Albano multiple maar (Alban Hills, Central Italy), *Bull. Volcanol.*, *68*, 567–591.

Frepoli, A., F. Marra, C. Magg, A. Marchetti, A. Nardi, N. M. Pagliuca, and M. Pirro (2010), Seismicity, seismogenic structures and crustal stress field in the greater area of Rome (Central Italy), *J. Geophys. Res.*, *115*, B12303, doi:10.1029/2009JB006322.

Funiciello, R., and M. Parotto (1978), Il substrato sedimentario nell'area dei Colli Albani: Considerazioni geodinamiche e paleogeografiche sul margine tirrenico dell'Appennino centrale, *Geologica Romana*, *17*, 233–287.

Gaeta, M., T. Di Rocco, and C. Freda (2009), Carbonate assimilation in open magmatic systems: The role of melt-bearing skarns and cumulate-forming processes, *J. Petrol.*, *50*, 361–385.

Gaeta, M., C. Freda, J. N. Christensen, L. Dallai, F. Marra, D. B. Karner, and P. Scarlato (2006), Evolution of the Mantle Source for Ultrapotassic Magmas of the Alban Hills Volcanic District (Central Italy), *Lithos*, *86*, 330–346, doi:10.1016/j.lithos.2005.05.010.

Gaeta, M., C. Freda, F. Marra, T. di Rocco, F. Gozzi, I. Arienzo, B. Giaccio, and P. Scarlato (2011), Petrology of the most recent ultrapotassic magmas from the Roman Province (Central Italy), *Lithos*, *127*(1-2), 298–308.

Gaeta, M., C. Freda, F. Marra, I. Arienzo, F. Gozzi, B. R. Jicha, and T. Di Rocco (2016), Paleozoic metasomatism at the origin of Mediterranean ultrapotassic magmas: Constraints from time-dependent geochemistry of Colli Albani volcanic products (Central Italy), *Lithos*, *244*, 151–164.

Giaccio, B., A. Sposato, M. Gaeta, F. Marra, D. M. Palladino, J. Taddeucci, M. Barbieri, P. Messina, and M. F. Rolfo (2007), Mid-distal occurrences of the Albano Maar pyroclastic deposits and their relevance for reassessing the eruptive scenarios of the most recent activity at the Colli Albani Volcanic District, Central Italy, *Quat Int.*, *171*, 160–178.

Giaccio, B., F. Marra, I. Hajdas, D. B. Karner, P. R. Renne, and A. Sposato (2009), $^{40}Ar/^{39}Ar$ and ^{14}C geochronology of the Albano maar deposits: Implications for defining the age and eruptive style of the most recent explosive activity at the Alban Hills Volcanic District, Italy, *J. Volcanol. Geotherm. Res.*, *185*(3), 203–213, doi:10.1016/j.jvolgeores.2009.05.011.

Giaccio, B., I. Arienzo, G. Sottili, F. Castorina, M. Gaeta, S. Nomade, P. Galli, and P. Messina (2013), Isotopic (Sr-Nd) and major element fingerprinting of distal tephras: An application to the Middle-Late Pleistocene markers from the Colli Albani volcano, central Italy, *Quat. Sci. Rev.*, *67*, 190–206.

Giordano, G., A. A. De Benedetti, A. Diana, G. Diano, F. Gaudioso, F. Marasco, M. Miceli, S. Mollo, R. A. F. Cas, and R. Funiciello (2006), The Colli Albani mafic caldera (Roma, Italy): Stratigraphy, structure and petrology, *J. Volcanol. Geotherm. Res.*, *155*, 49–80.

Gozzi, F., M. Gaeta, C. Freda, S. Mollo, T. Di Rocco, F. Marra, L. Dallai, and A. Pack (2014), Primary magmatic calcite reveals origin from crustal carbonate, *Lithos*, *190-191*, 191–203.

Jicha, B. R., B. S. Singer, and P. Sobol (2016), Re-evaluation of the ages of $^{40}Ar/^{39}Ar$ sanidine standards and supereruptions in the western U.S. using a Noblesse multi-collector mass spectrometer, *Chem. Geol.*, *431*, 54–66, doi:10.1016/j.chemgeo.2016.03.024.

Karner, D. B., and P. R. Renne (1998), 40Ar/39Ar geochronology of Roman volcanic province tephra in the Tiber River Valley: Age calibration of middle Pleistocene sea-level changes, *Geol. Soc. Am. Bull.*, *110*, 740–747.

Karner, D. B., F. Marra, and P. Renne (2001a), The history of the Monti Sabatini and Alban hills volcanoes: Groundwork for assessing volcanic-tectonic hazards for Rome, *J. Volcanol. Geotherm. Res.*, *107*, 185–219.

Karner, D. B., F. Marra, F. Florindo, and E. Boschi (2001b), Pulsed uplift estimated from terrace elevations in the coast of Rome: Evidence for a new phase of volcanic activity?, *Earth Planet. Sci. Lett.*, *188*, 135–148.

Marra, F. (1999), Low-magnitude earthquakes in Rome: Structural interpretation and implications for local stress-field, *Geophys. J. Int.*, *138*, 231–243.

Marra, F. (2001), Strike-slip faulting and block rotation: A possible triggering mechanism for lava flows in the Alban Hills?, *J. Struct. Geol.*, *23*(2), 129–141.

Marra, F., C. Freda, P. Scarlato, J. Taddeucci, D. B. Karner, P. R. Renne, M. Gaeta, D. M. Palladino, R. Trigila, and G. Cavarretta (2003), Post-caldera activity in the Alban hills volcanic district (Italy): 40Ar/39Ar geochronology and insights into magma evolution, *Bull. Volcanol.*, *65*, 227–247.

Marra, F., J. Taddeucci, C. Freda, W. Marzocchi, and P. Scarlato (2004a), Recurrence of volcanic activity along the Roman comagmatic province (Tyrrhenian margin of Italy) and its tectonic significance, *Tectonics*, *23*, TC4013, doi:10.1029/2003TC001600.

Marra, F., P. Montone, M. Pirro, and E. Boschi (2004b), Evidence of active tectonics on a Roman aqueduct system (II-III Century A.D.) near Rome, Italy, *J. Struct. Geol.*, *26*, 679–690.

Marra, F., D. B. Karner, C. Freda, M. Gaeta, and P. R. Renne (2009), Large mafic eruptions at the Alban Hills Volcanic District (Central Italy): Chronostratigraphy, petrography and eruptive behavior, *J. Volcanol. Geotherm. Res.*, *179*, 217–232, doi:10.1016/j.jvolgeores.2008.11.009.

Montone, P., A. Amato, C. Chiarabba, G. Buonasorte, and A. Fiordelisi (1995), Evidence of active extension in Quaternary volcanoes of Central Italy from breakout analysis and seismicity, *Geophys. Res. Lett.*, *22*, 1909–1912, doi:10.1029/95GL01326.

Peccerillo, A. (2005), *Plio-Quaternary Volcanism in Italy: Petrology, Geochemistry, Geodynamics*, Springer, Berlin.

Rivera, T. A., M. Storey, M. D. Schmitz, and J. L. Crowley (2013), Age intercalibration of $^{40}Ar/^{39}Ar$ sanidine and chemically distinct U/Pb zircon populations from the Alder Creek Rhyolite Quaternary geochronology standard, *Chem. Geol.*, *345*, 87–98.

Salvi, S., S. Atzori, C. Tolomei, J. Allievi, A. Ferretti, F. Rocca, C. Prati, S. Stramondo, and N. Feuillet (2004), Inflation rate of the Colli Albani volcanic complex retrived by the permanent scatters SAR interferometry technique, *Geophys. Res. Lett.*, *31*, L12606, doi:10.1029/2004GL020253.

Sottili, G., J. Taddeucci, D. M. Palladino, M. Gaeta, P. Scarlato, and G. Ventura (2009), Sub-surface dynamics and eruptive styles of maars in the Colli Albani Volcanic District, Central Italy, *J. Volcanol. Geotherm. Res.*, *180*, 189–202.

Stramondo, S., F. Bozzano, F. Marra, U. Wegmuller, F. R. Cinti, M. Moro, and M. Saroli (2008), Subsidence induced by urbanisation in the city of Rome detected by advanced InSAR technique and geotechnical investigations, *Remote Sens. Environ.*, *112*, 3160–3172, doi:10.1016/j.rse.2008.03.008.

Werner, C., U. Wegmuller, T. Strozzi, and A. Wiesmann (2003), Interferometric point target analysis for deformation mapping, in *Proceedings of IGARSS '03*, vol. 7, pp. 4362–4364, IEEE International.